**Earthquakes and Structures**, *Vol. 17, No. 3* (*2019*) *329-336*
DOI: https://doi.org/10.12989/eas.2019.17.3.329


# Thermal vibration analysis of FGM beams using an efficient shear deformation beam theory

Abdelkader Safa[1,2], Lazreg Hadji*[3,4], Mohamed Bourada[2] and Nafissa Zouatnia[5]

[1]*Department of Civil Engineering, Ahmed Zabana University Centre, Relizane, 48000, Algeria*
[2]*Material and Hydrology Laboratory, University of Sidi Bel Abbes, Faculty of Technology, Civil Engineering Department, Sidi Bel Abbes, Algeria*
[3]*Department of Mechanical Engineering, Ibn Khaldoun University, BP 78 Zaaroura, 14000, Tiaret, Algeria*
[4]*Laboratory of Geomatics and Sustainable Development, Ibn Khaldoun University of Tiaret, Algeria*
[5]*Department of Civil Engineering, Ibn Khaldoun University, BP 78 Zaaroura, Tiaret, 14000, Algeria*

(*Received April 4, 2019, Revised August 2, 2019, Accepted August 3, 2019*)

**Abstract.** An efficient shear deformation beam theory is developed for thermo-elastic vibration of FGM beams. The theory accounts for parabolic distribution of the transverse shear strains and satisfies the zero traction boundary conditions on the on the surfaces of the beam without using shear correction factors. The material properties of the FGM beam are assumed to be temperature dependent, and change gradually in the thickness direction. Three cases of temperature distribution in the form of uniformity, linearity, and nonlinearity are considered through the beam thickness. Based on the present refined beam theory, the equations of motion are derived from Hamilton's principle. The closed-form solutions of functionally graded beams are obtained using Navier solution. Numerical results are presented to investigate the effects of temperature distributions, material parameters, thermal moments and slenderness ratios on the natural frequencies. The accuracy of the present solutions is verified by comparing the obtained results with the existing solutions.

**Keywords:** thermo-elastic vibration; functionally graded materials; Hamilton's principle; Navier solution

## 1. Introduction

Functionally graded materials (FGMs) have many advantages for use in engineering structural components. Unlike fiber-matrix laminated composites, FGMs do not have problems of de-bonding and delaminating that result from large inter-laminar stresses. The concept of FGMs was initially introduced in the mid-1980s by Japanese scientists. FGMs are designed so that material properties vary smoothly and continuously through the thickness from the surface of a ceramic exposed to high temperature to that of a metal on the other surface. The composition of the material changes gradually throughout the thickness direction. The FGMs are widely used in mechanical, aerospace, nuclear, and civil engineering. Consequently, studies devoted to understand the thermo-elastic vibration of FGM beams have being paid more and more attentions in recent years. Sankar and Tzeng (2002) used CBT to study the thermal stresses of simply supported FG beams. Wattanasakulpong *et al.* (2011) studied the thermal buckling and elastic vibration of third-order shear deformable functionally graded beams. Giunta *et al.* (2013) developed Navier solution to analyse the static behaviour of FG beams under thermo-mechanical loads. Trinh *et al.* (2016) developed an analytical method for the vibration and buckling of functionally graded beams under mechanical and thermal loads. Recently, Mouli *et al.* (2018) investigated the numerical study of temperature dependent eigenfrequency responses of tilted functionally graded shallow shell structures. Bennai *et al.* (2018) developed the dynamic and wave propagation investigation of FGM plates with porosities using a four variable plate theory. Ebrahimi *et al.* (2018) analyze the vibration of inhomogeneous nonlocal beams via a modified couple stress theory incorporating surface effects. Hamdi *et al.* (2018) developed the beam finite element model of a vibrate wind blade in large elastic deformation. Rong *et al.* (2018) used an analytical solution for natural frequency of monopile supported wind turbine towers. Wu *et al.* (2018) studied the free vibration of thermo-electro-mechanically postbuckled FG-CNTRC beams with geometric imperfections. Chen *et al.* (2018) studied the thermal vibration of FGM beams with general boundary conditions using a higher-order shear deformation theory. Menasria *et al.* (2017) developed a new and simple HSDT for thermal stability analysis of FG sandwich plates. El-Haina *et al.* (2017) used a simple analytical approach for thermal buckling of thick functionally graded sandwich plates. Attia *et al.* (2018) used a refined four variable plate theory for thermoelastic analysis of FGM plates resting on variable elastic foundations. Karami *et al.* (2018) investigated a size-dependent quasi-3D model for wave dispersion analysis of FG nanoplates. Karami *et al.* (2018) studied a size-dependent quasi-3D model for wave dispersion analysis of FG nanoplates. Semmah *et al.* (2019) studied thermal buckling analysis of SWBNNT on Winkler foundation by

*Corresponding author, Ph.D.
E-mail: had_laz@yahoo.fr



ISSN: 2092-7614 (Print), 2092-7622 (Online)

Table 1 Temperature dependent coefficient of the materials

| Materials | Properties | $P_0$ | $P_{-1}$ | $P_1$ | $P_2$ | $P_3$ |
|---|---|---|---|---|---|---|
| $Al_2O_3$ | $E$ (Pa) | 349.55e$^{+9}$ | 0 | -3.853e$^{-4}$ | 4.027e$^{-7}$ | -1.673e$^{-10}$ |
| | $\alpha$ (1/K) | 6.8269e$^{-6}$ | 0 | 1.838e$^{-4}$ | 0 | 0 |
| | $k$ (W/mK) | -14.087 | -1123.6 | -6.227e$^{-3}$ | 0 | 0 |
| | $\nu$ | 0.26 | 0 | 0 | 0 | 0 |
| | $\rho$ (kg/m$^3$) | 3800 | 0 | 0 | 0 | 0 |
| $Si_3N_4$ | $E$ (Pa) | 348.43e$^{+9}$ | 0 | -3.070e$^{-4}$ | 2.160e$^{-7}$ | -87946e$^{-11}$ |
| | $\alpha$ (1/K) | 5.8723e$^{-6}$ | 0 | 9.095e$^{-4}$ | 0 | 0 |
| | $k$ (W/mK) | 13.723 | 0 | -1.032e$^{-3}$ | 5.466e$^{-7}$ | -7.876e$^{-11}$ |
| | $\nu$ | 0.24 | 0 | 0 | 0 | 0 |
| | $\rho$ (kg/m$^3$) | 2370 | 0 | 0 | 0 | 0 |
| SUS304 | $E$ (Pa) | 2.01e$^{+11}$ | 0 | 3.08e$^{-04}$ | -6.534e$^{-7}$ | 0 |
| | $\alpha$ (1/K) | 1.233e$^{-05}$ | 0 | 8.086e$^{-4}$ | 0 | 0 |
| | $k$ (W/mK) | 15.379 | 0 | -1.264e$^{-3}$ | 2.092e$^{-6}$ | -7.223e$^{-10}$ |
| | $\nu$ | 0.3262 | 0 | -2.002e$^{-4}$ | 3.797e$^{-7}$ | 0 |
| | $\rho$ (kg/m$^3$) | 8166 | 0 | 0 | 0 | 0 |

non local FSDT.

It should be noted that the thickness stretching effect is neglected in these new three variable beam theories and the transverse displacement is considered constant in the thickness direction. The thickness stretching effect in functionally graded structures has been pointed and discussed out recently by many researchers (Khelifa *et al.* 2018, Abualnour *et al.* 2018, Bouhadra *et al.* 2018, Boukhlif *et al.* 2019, Boulefrakh *et al.* 2019).

In this paper, a refined beam theory is proposed for the thermo-elastic vibration of FGM beam. First, temperature dependant and functionally graded material properties of the beam are stated in mathematical forms. Second, uniform, linear, and nonlinear temperature distributions through the beam thickness are introduced. Third, the present refined beam theory is introduced and compared with several theories. Equations of motion derived from Hamilton's principle. The effects of the temperature rise, material parameters, thermal moments and slenderness ratios on the free vibration characteristics of FGM beam are studied accordingly. The accuracy and effectiveness of proposed theory are verified by comparison with previous research.

## 2. Problem formulation

### *2.1 Material properties of temperature dependent FGM beam*

A FG beam made by ceramic-metal is considered in this investigation. The beam has length ($L$), width ($b$) and thickness ($h$).

The material composition at the top surface ($z=h/2$) is assumed to be the ceramic-rich and it is varying continuously to the metal-rich surface at the opposite side ($z=-h/2$). The geometry of the FG beam is shown in Fig. 1. The power law distribution is used for the volume Fraction of the ceramic ($V_c$) and the metal ($V_m$) as

$$V_c(z)=\left(\frac{z}{h}+\frac{1}{2}\right)^k,\ V_m(z)=1-V_c(z) \tag{1}$$

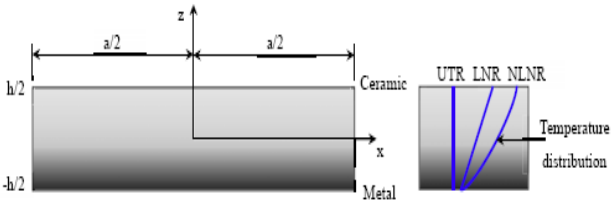


Fig. 1 Geometry and coordinate of a FG beam

where $k$ is the material parameter.

The thermo-elastic material properties are considered as a function of temperature $T$ and can be calculated for ceramic and metal (Shen *et al*. 2014)

$$P(T)=P_0\left(P_{-1}T^{-1}+1+P_1T+P_2T^2+P_3T^3\right) \tag{2}$$

Where $P$ denotes Young's modulus $E$, mass density $\rho$ and thermal expansion coefficient $\alpha$, respectively. $P_0$, $P_{-1}$,$P_1$, $P_2$ and $P_3$ are the temperature dependent coefficients, which are listed in Table 1 for various materials. Fig. 2 presents the material properties of ceramics and metals with respect to the temperature change. Based on the power rule together with the temperature-dependence described in Eq. (2), the typical material properties $P(z,T)$ of beam through the thickness are described as

$$P(z,T)=\left[P_c(T-P_m(T))\right]V_c(z)+P_m(T) \tag{3}$$

The material properties are calculated by Eq. (2) for ceramic and metal at the specific temperature and followed by Eq. (3) to obtain the values at $z$. It should be noticed that the Poisson's ratio $\nu$ is evaluated as the average of ceramic and metal values at $T_0$=300K.

### *2.2 Various cases of temperature distribution*

#### *2.2.1 Uniform temperature distribution (UTD)*

The temperature of the whole beam is assumed uniform and increased from $T_0$=300K to the current value. It means that the temperature at a point is $T(z)=T_0+\Delta T$, where $\Delta T$ is the temperature rise.

Where $T_0$ denotes the ambient temperature, under which the FGM beam is in a stress-free state.

### *2.2.2 Nonlineair temperature distribution (NLTD)*

Assume that the temperature on the top and bottom surfaces of FGM beam remain constant, and are marked as $T_c$ and $T_m$. Using the heat conduction rule, we can obtain a steady state equation as follows

$$-\frac{d}{dz}\left[k(z)\frac{dT}{dz}\right]=0,\quad \begin{cases} T=T_m, z=-h/2 \\ T=T_c, z=h/2 \end{cases} \tag{4}$$

The temperature function $T(z)$ can be obtained with the first seven terms of the polynomial series (Javaheri and Eslami 2002)

$$T(z)=T_m+\frac{\Delta T}{C}\left[\begin{array}{l} \left(\frac{z}{h}+\frac{1}{2}\right)-\frac{k_{cm}}{(k+1)k_m}\left(\frac{z}{h}+\frac{1}{2}\right)^{k+1}+ \\ \frac{k_{cm}^2}{(2k+1)k_m^2}\left(\frac{z}{h}+\frac{1}{2}\right)^{2k+1}-\frac{k_{cm}^3}{(3k+1)k_m^3}\left(\frac{z}{h}+\frac{1}{2}\right)^{3k+1} \\ +\frac{k_{cm}^4}{(4k+1)k_m^4}\left(\frac{z}{h}+\frac{1}{2}\right)^{4k+1}-\frac{k_{cm}^5}{(5k+1)k_m^5}\left(\frac{z}{h}+\frac{1}{2}\right)^{5k+1} \end{array}\right] \tag{5}$$

with

$$C=1-\frac{k_{cm}}{(p+1)k_m}+\frac{k_{cm}^2}{(2p+1)k_m^2}-\frac{k_{cm}^3}{(3p+1)k_m^3} +\frac{k_{cm}^4}{(4p+1)k_m^4}-\frac{k_{cm}^5}{(5p+1)k_m^5} \tag{6}$$

$$k_{cm}=k_c-k_m,\ \Delta T=T_c-T_m \tag{7}$$

Where $k_c$ and $k_m$ represent the thermal conductivity of ceramic and metal under the surface temperatures.

### *2.2.3 Lineair temperature distribution (LTD)*

The temperature in the ceramic and metal faces of FG beam is assumed to be $T_c$ and $T_m$. In this case, the temperature on the metal surface is supposed to be $T_m$=305K, whereas on the ceramic surface it is surged to $T_c=T_0+\Delta T$. With the assumption of linear distribution, the temperature through the thickness can be determined as

$$T(z)=T_m+\Delta T\left(\frac{1}{2}+\frac{z}{h}\right) \tag{8}$$

## *2.3 Kinematics*

Based on a generalized higher-order shear deformation theory, the displacement field of the considered beam can be expressed as

$$u(x,z,t)=u_0(x,t)-z\frac{\partial w_b}{\partial x}-f(z)\frac{\partial w_s}{\partial x} \tag{9a}$$

$$w(x,z,t)=w_b(x,t)+w_s(x,t) \tag{9b}$$

Where $u_0$ is the axial displacement of a point on the midplane of the beam; $w_b$ and $w_s$ are the bending and shear components of transverse displacement of a point on the midplane of the beam; and $f(z)$ is a shape function determining the distribution of the transverse shear strain and shear stress through the depth of the beam. The shape functions $f(z)$ is chosen to satisfy the stress-free boundary conditions on the top and bottom surfaces of the beam, thus a shear correction factor is not required. In this work, the present refined beam theory is obtained by setting

$$f(z)=\frac{4}{3}\frac{z^3}{h^2} \tag{10}$$

The strains associated with the displacements in Eq. (9) are

$$\varepsilon_x=\varepsilon_x^0+z\,k_x^b+f(z)\,k_x^s \tag{11a}$$

$$\gamma_{xz}=g(z)\,\gamma_{xz}^s \tag{11b}$$

where

$$\varepsilon_x^0=\frac{\partial u_0}{\partial x},k_x^b=-\frac{\partial^2 w_b}{\partial x^2},k_x^s=-\frac{\partial^2 w_s}{\partial x^2},\gamma_{xz}^s=\frac{\partial w_s}{\partial x} \tag{11c}$$

$$g(z)=1-f'(z)\ \text{ and }\ f'(z)=\frac{df(z)}{dz} \tag{11d}$$

The state of stress in the beam is given by the generalized Hooke's law as follows

$$\sigma_x=Q_{11}(z)\,\varepsilon_x\ \text{ and }\ \tau_{xz}=Q_{55}(z)\,\gamma_{xz} \tag{12a}$$

where

$$Q_{11}(z)=E(z,T)\ \text{ and }\ Q_{55}(z)=\frac{E(z,T)}{2(1+\nu(z,T))} \tag{12b}$$

## *2.4 Equations of motion*

The total strain energy of FG beam is given by

$$U=U_P+U_T \tag{13}$$

where $U_p$ and $U_T$ are the strain energies due to mechanical and thermal effects, respectively. The strain energies $U_p$ and $U_T$ are given by (Shahrjerdi *et al.* 2011, Li *et al.* 2009)

$$U_P=\int_0^L\int_{-\frac{h}{2}}^{\frac{h}{2}}\left(\sigma_x\delta\varepsilon_x+\tau_{xz}\delta\gamma_{xz}\right)dzdx \tag{14a}$$

$$U_T=\int_0^L\int_{-\frac{h}{2}}^{\frac{h}{2}}\left(\sigma_x^T d_{11}\right)dzdx \tag{14b}$$

Where $d_{ij}$ ($i$,$j$=1) ($i$, $j$=1) is the nonlinear strain-displacement relationship (Shahrjerdi *et al.* 2011, Reddy 2004). By substituting $d_{ij}$ into Eq. (14b) the following equation is obtained

$$U_T=\int_0^L\int_{-\frac{h}{2}}^{\frac{h}{2}}\sigma_x^T\left[\left(\frac{\partial u}{\partial x}\right)^2+\left(\frac{\partial w}{\partial x}\right)^2\right]dzdx \tag{15a}$$

with

$$\sigma_x^T=-E(z,T)\alpha(z,T)\Delta T(z) \tag{15b}$$

The kinetic energy of plate is given by

$$K=\frac{1}{2}\int_0^L\int_{-h/2}^{h/2}\rho(z,T)\left[\dot{u}+\dot{w}\right]dzdx \tag{16}$$

Hamilton's principle for an elastic body can be represented as

$$\delta\int_{t_1}^{t_2}(U-K)dt=0 \tag{17}$$

By substituting Eq. (11) into Eq. (12) and applying Eqs. (17) and (9), equations of motion for FG beam can be obtained as follows

$$\begin{aligned}&\left(A_{11}+A_{11}^T\right)d_{11}u_0-\left(B_{11}+B_{11}^T\right)d_{111}w_b\\&-\left(B_{11}^s+B_{11}^{sT}\right)d_{111}w_s=I_0\ddot{u}_0-I_1d_1\ddot{w}_b\\&-J_1d_1\ddot{w}_s\end{aligned} \tag{18a}$$

$$\begin{aligned}&\left(B_{11}+B_{11}^T\right)d_{111}u_0-\left(D_{11}+D_{11}^T\right)d_{1111}w_b\\&-\left(D_{11}^s+D_{11}^{sT}\right)d_{1111}w_s+A_{11}^T\left(d_{11}w_b+d_{11}w_s\right)\\&=I_0\left(\ddot{w}_b+\ddot{w}_s\right)+I_1d_1\ddot{u}_0-I_2d_{11}\ddot{w}_b-J_2d_{11}\ddot{w}_s\end{aligned} \tag{18b}$$

$$\begin{aligned}&\left(B_{11}^s+B_{11}^{sT}\right)d_{111}u_0-\left(D_{11}^s+D_{11}^{sT}\right)d_{1111}w_b\\&-\left(H_{11}^s+H_{s11}^T\right)d_{1111}w_s+A_{55}^sd_{11}w_s+A_{11}^T\left(d_{11}w_b+d_{11}w_s\right)\\&=I_0\left(\ddot{w}_b+\ddot{w}_s\right)+J_1d_1\ddot{u}_0-J_2d_{11}\ddot{w}_b-K_2d_{11}\ddot{w}_s\end{aligned} \tag{18c}$$

where $d_{ij}$, $d_{ijl}$ and $d_{ijlm}$ are the following differential operators

$$\begin{aligned}&d_{ij}=\frac{\partial^2}{\partial x_i\partial x_j},\ d_{ijl}=\frac{\partial^3}{\partial x_i\partial x_j\partial x_l},\\&d_{ijlm}=\frac{\partial^4}{\partial x_i\partial x_j\partial x_l\partial x_m},\quad d_i=\frac{\partial}{\partial x_i},\quad (i,j,l,m=1)\end{aligned} \tag{19}$$

and stiffness components are given as

$$\left(A_{11},B_{11},D_{11},B_{11}^s,D_{11}^{sT},H_{11}^{sT}\right)=\int_{-\frac{h}{2}}^{\frac{h}{2}}Q_{11}\left(1,z,z^2,f(z),z\,f(z),f^2(z)\right)dz \tag{20a}$$

$$A_{55}^s=\int_{-\frac{h}{2}}^{\frac{h}{2}}Q_{55}\left[g(z)\right]^2dz \tag{20b}$$

$$\left(A_{11}^T,B_{11}^T,D_{11}^T,B_{11}^{sT},D_{11}^s,H_{11}^s\right)=\int_{-\frac{h}{2}}^{\frac{h}{2}}\sigma_x^T\left(1,z,z^2,f(z),z\,f(z),f^2(z)\right)dz \tag{20c}$$

The inertias are also defined as

$$\left(I_0,I_1,J_1,I_2,J_2,K_2\right)=\int_{-\frac{h}{2}}^{\frac{h}{2}}\left(1,z,f,z^2,zf,f^2\right)\rho(z)dz \tag{21}$$

## 3. Analytical solutions

Based on the Navier approach with simply supported boundary conditions, the displacement fields are expressed as

$$\begin{Bmatrix}u_0\\w_b\\w_s\end{Bmatrix}=\sum_{m=1}^{\infty}\begin{Bmatrix}U_m\cos(\lambda x)e^{i\omega t}\\W_{bm}\sin(\lambda x)e^{i\omega t}\\W_{sm}\sin(\lambda x)e^{i\omega t}\end{Bmatrix} \tag{22}$$

where $U_m$, $W_{bm}$, and $W_{sm}$ are arbitrary parameters to be determined, $\omega$ is the eigenfrequency associated with $m$ th eigenmode, and $\lambda=m\pi/L$.

Substituting the displacement fields (22) into equations of motion (18), the following frequency equation is obtained

$$\left(\begin{bmatrix}a_{11}&a_{12}&a_{13}\\a_{12}&a_{22}&a_{23}\\a_{13}&a_{23}&a_{33}\end{bmatrix}-\omega^2\begin{bmatrix}m_{11}&m_{12}&m_{13}\\m_{12}&m_{22}&m_{23}\\m_{13}&m_{23}&m_{33}\end{bmatrix}\right)\begin{Bmatrix}U_m\\W_{bm}\\W_{sm}\end{Bmatrix}=\begin{Bmatrix}0\\0\\0\end{Bmatrix} \tag{23}$$

in which

$$\begin{aligned}a_{11}&=-\left(A_{11}+A_{11}^T\right)\lambda^2\\a_{12}&=\left(B_{11}+B_{11}^T\right)\lambda^3\\a_{13}&=\left(B_{11}^s+B_{11}^{sT}\right)\lambda^3\\a_{22}&=-\left[\left(D_{11}+D_{11}^T\right)\lambda^4+A_{11}^T\lambda^2\right]\\a_{23}&=-\left[\left(D_{11}^s+D_{11}^{sT}\right)\lambda^4+A_{11}^T\lambda^2\right]\\a_{33}&=-\left[\left(H_{11}^s+H_{11}^{sT}\right)\lambda^4+\lambda^2\left(A_{55}^s+A_{11}^T\right)\right]\end{aligned} \tag{24a}$$

and

$$\begin{aligned}m_{11}&=I_1\\m_{12}&=I_1\lambda\\m_{13}&=J_1\lambda\\m_{22}&=-\left(I_0+I_2\lambda^2\right)\\m_{23}&=-\left(I_0+J_2\lambda^2\right)\\m_{33}&=\left(I_0+K_2\lambda^2\right)\end{aligned} \tag{24b}$$

## 4. Numerical results

### *4.1 Free vibration results of FG beams without thermal effects*

The theoretical formulation in this paper is verified by setting $\Delta T$=0 and then comparing free vibration results of FG beams without thermal effects with Sina *et al.* (2009) and Simsek (2010). Sina *et al.* (2009) show more accuracy can be obtained from the developed first order theory FSDT1 than that of the traditional first order theory FSDT2 in order to predict frequency results of FG beams. In their research, the FG beams made of Al/$Al_2O_3$ that the Al rich is set at the top surface, whereas the opposite surface is the $Al_2O_3$ rich, whose material properties are:

Al : $E_m$=70 GPa, $\rho_m$=2700 kg/m$^3$, $\nu_m$=0.23,

Table 2 Dimensionless fundamental frequency $\Omega = \omega \frac{L^2}{h}\sqrt{\frac{I_0}{\int_{-h/2}^{h/2} E(z)dz}}$ of Al/$Al_2O_3$ beams with $p$=0.3 under ambient temperature

| Source | $L/h$=10 | $L/h$=30 | $L/h$=100 |
|---|---|---|---|
| Present | 2.776 | 2.813 | 2.817 |
| Wattanasakulpong *et al.* (2011) | 2.803 | 2.845 | 2.85 |
| FSDBT1 (Sina *et al.* 2009) | 2.774 | 2.813 | 2.817 |
| FSDBT2 (Sina *et al.* 2009) | 2.695 | 2.737 | 2.742 |
| PSDBT Simsek (2010) | 2.702 | 2.738 | 2.742 |
| ASDBT Simsek (2010) | 2.702 | 2.738 | 2.742 |

Table 3 Fundamental frequency with respect to the temperature rise of $Al_2O_3$/SUS304 beams under UTD ($L/h$=30)

| Theory | | $p$=0.2 | | | $p$=2 | | |
|---|---|---|---|---|---|---|---|
| | | $\Delta T$=0 | $\Delta T$=50 | $\Delta T$=100 | $\Delta T$=0 | $\Delta T$=50 | $\Delta T$=100 |
| TID | Trinh *et al.* (2016) | 2.9506 | 1.8450 | - | 3.0129 | 1.1816 | - |
| TD | Trinh *et al.* (2016) | 2.9506 | 1.8220 | - | 3.0129 | 1.0868 | - |
| | Present | 2.9454 | 1.8146 | - | 2.9892 | 1.0292 | - |

$Al_2O_3$ : $E_m$=380 GPa, $\rho_c$=3800 kg/m$^3$, $v_c$=0.23,

The dimensionless frequency for the FG beam can be expressed as

$$\Omega = \omega L^2 \sqrt{\frac{I_0}{h^2 \int_{-h/2}^{h/2} E(z)dz}} \tag{25}$$

From Table 2, it is observed that the agreement is satisfactory in comparisons with the present frequency results and those from the published results for various slenderness ratio $L/h$, especially when comparing with the developed theory FSDT1.

### *4.2 Free vibration results of FG beams without thermal moments*

From the extensive literature review on this research topic, it is clear that there are no results available on the free vibration analysis of the heated beams without thermal moments (except the results of Trinh *et al.* 2016). In the case where the thermal moment is zero, it means that the thermal stiffness components $\left(B_{11}^T, D_{11}^T, B_{11}^{sT}, D_{11}^s, H_{11}^s\right) = 0$. This example also aims to verify the thermal effect of the properties of temperature independent materials (TID) and temperature dependence (TD). Table 3 present the fundamental frequency with respect to the temperature rise of $Al_2O_3$/SUS304 beams under UTD without thermal moments. This table reveal that the TD gives significantly lower values compared to TID one, which highlights the importance of temperature dependence in FG beams. Due to this reason, only TD solution is used in the rest of the paper. Also, the difference between the results of the present theory and the results of Luan *et al.* (2016) is very clear in this table. This difference is due to the negligence of the thermal moment effect in the FGM beam.

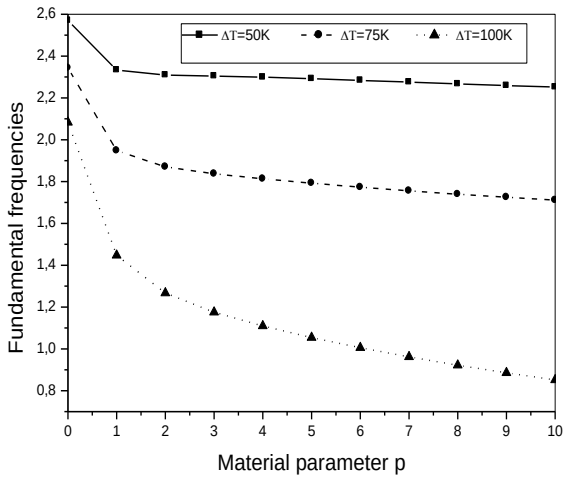


Fig. 2 The fundamental frequency-parameter curves of S-S $Si_3N_4$/SUS304 beams with different temperatures $L/h$=20

### *4.3 FGM beams with UTD*

Thermal vibration analysis of FGM beam of $Al_2O_3$/SUS304 with UTD are presented in this section. The properties of these temperature-dependent materials are listed in Table 1. To verify with the results provides by Chen *et al.* (2018), the elastic coefficients, $Q_{11} = \frac{E(z)}{(1-\nu^2)}$ and $Q_{55} = \frac{E(z)}{2(1+\nu)}$, are used in this example, and the thermal stresses are expressed as $\sigma_x^T = -\frac{E(z)\alpha(z)\Delta T}{(1-\nu)}$. The following dimensionless natural frequencies are used $\Omega = \omega \frac{L^2}{h}\sqrt{I_0 / \int_{-h/2}^{h/2} E(z)dz}$

The first five dimensionless frequencies of $Al_2O_3$/SUS304 beams with $p$=0.2 and 2 ($L/h$=20) with respect to uniform temperature rise are shown in Table 4. It can be seen that the results obtained with the present refined beam theory match well with the reference data. Also, As the temperature increases, the fundamental frequencies decrease.

The effects of material parameter p on the fundamental frequencies of Si3N4/SUS304 beams ($L/h$=20) with different temperatures are depicted in Fig. 2. We can observed that the natural frequencies of the FGM beam decrease with the increase of the material parameter. The influence of the uniform temperature change $\Delta T$ on the fundamental frequencies of $Si_3N_4$/SUS304 beams ($L/h$=20) with various material parameter are shown in Fig. 3. It can be seen that the fundamental dimensionless frequencies of the FGM beams decrease as the temperature increases.

### *4.4 FGM beams with LTD and NLTD*

The comparison between UTR and LNR solutions as

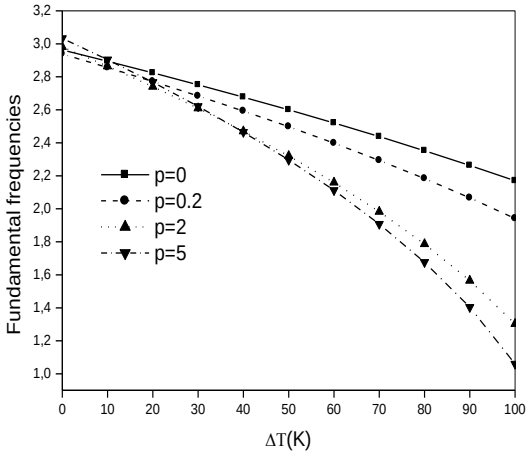


Fig. 3 The first temperature-frequency curves of S-S $Si_3N_4$/SUS304 beams ($L/h$=20)

well as LNR and NLNR solutions for the natural frequencies of FG beams is given in Tables 5-6. The following dimensionless natural frequency is used

$$\overline{\Omega} = \omega L^2 \sqrt{\frac{\rho_c A}{E_c I}} \tag{26}$$

In wich $\rho_c$ and $E_c$ are the density and Young's modulus of the ceramic material at ambient temperature. The results reported by Trinh *et al*. (2016) for the case of S-S beams using the TSDBT and Ebrahimi *et al.* (2015), Chen *et al.* (2018) are also given for the verification purpose. A good agreement between the present results with previous ones can be observed for various $p$ values. For all material parameters, the LTD results are significantly greater than those from the UTD.

The thermo-elastic vibration characteristic of the simply FGM beams under LTD and NLTD with different material

Table 4 First five dimensionless frequencies of *P-P* $Al_2O_3$/SUS304 under UTD

| Modes | Theory | $p$=0.2 | | | $p$=2 | | |
|---|---|---|---|---|---|---|---|
| | | $\Delta T$=0 | $\Delta T$=100 | $\Delta T$=200 | $\Delta T$=0 | $\Delta T$=100 | $\Delta T$=200 |
| 1 | Chen *et al.* (2018) | 2.941 | 1.946 | - | 3.003 | 1.348 | - |
| | Present | 2.938 | 1.942 | 1.178 | 2.982 | 1.303 | 2.496 |
| 2 | Chen *et al.* (2018) | 11.601 | 10.731 | 9.719 | 11.766 | 10.473 | 8.830 |
| | Present | 11.601 | 10.731 | 9.719 | 11.767 | 10.474 | 8.831 |
| 3 | Chen *et al.* (2018) | 25.569 | 24.700 | 23.736 | 25.935 | 24.656 | 23.163 |
| | Present | 25.566 | 24.697 | 23.733 | 25.916 | 24.636 | 23.141 |
| 4 | Chen *et al.* (2018) | 44.225 | 43.340 | 42.367 | 44.760 | 43.462 | 41.975 |
| | Present | 44.230 | 43.346 | 42.373 | 44.799 | 43.498 | 42.010 |
| 5 | Chen *et al.* (2018) | 65.621 | 65.583 | 65.006 | 65.560 | 65.500 | 64.860 |
| | Present | 66.911 | 66.001 | 65.003 | 67.710 | 66.373 | 64.854 |

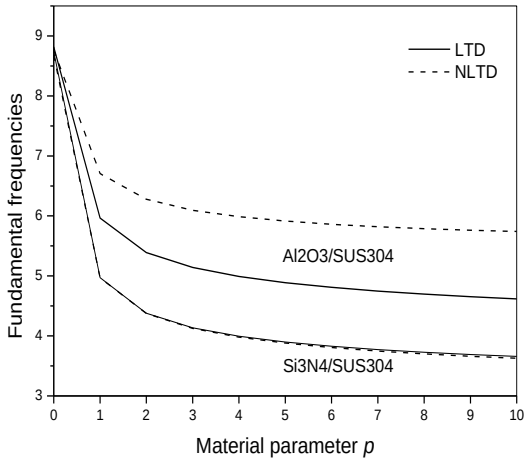


Fig. 4 Fundamental frequency of FGM beams under LTD and NLTD with different material parameter ($\Delta T$=100K), ($L/h$=20)

Table 5 Dimensionless natural frequencies of *P-P* $Si_3N_4$/SUS304 beams under UTD and LTD ($L/h$=20)

| $\Delta T$ | Mode | Theory | UTD | | | LTD | | |
|---|---|---|---|---|---|---|---|---|
| | | | $p$=0 | 1 | 5 | $p$=0 | 1 | 5 |
| 10 | 1 | Trinh *et al.* (2016) | 2.8842 | 2,8450 | 2,9109 | 9.6843 | 5.8432 | 4.7454 |
| | | Present | 2.8831 | 2.8242 | 2.8966 | 9.6839 | 5.8043 | 4.7243 |
| | 2 | Trinh *et al.* (2016) | 11.5991 | 11,4678 | 11,8148 | 38.6698 | 23.2942 | 19.0058 |
| | | Present | 11.5920 | 11.4640 | 11.8077 | 38.6686 | 23.2954 | 19.0055 |
| | 3 | Trinh *et al.* (2016) | 25.6350 | 25,4240 | 26,1669 | 85.4928 | 51.5782 | 42.0626 |
| | | Present | 25.6336 | 25.3889 | 26.1501 | 85.4903 | 51.5401 | 42.0407 |
| 30 | 1 | Trinh *et al.* (2016) | 2,7347 | 2,6157 | 2,6324 | 9.4864 | 5.6727 | 4.5792 |
| | | Present | 2.7332 | 2.5937 | 2.6156 | 9.4857 | 5.6332 | 4.5576 |
| | 2 | Trinh *et al.* (2016) | 11,4594 | 11.2543 | 11,5484 | 38.4431 | 23.1103 | 18.8315 |
| | | Present | 11.4458 | 11.2448 | 11.5415 | 38.4404 | 23.1103 | 18.8301 |
| | 3 | Trinh *et al.* (2016) | 25,4885 | 25,1915 | 25,9057 | 85.2146 | 51.3662 | 41.8680 |
| | | Present | 25.4855 | 25.1686 | 25.8801 | 85.2089 | 51.3264 | 41.8443 |
| 60 | 1 | Trinh *et al.* (2016) | 2,4845 | 2,2158 | 2,1295 | 9.1774 | 5.4030 | 4.3136 |
| | | Present | 2.4827 | 2.18907 | 2.1082 | 9.17601 | 5.3625 | 4.2911 |
| | 2 | Trinh *et al.* (2016) | 11,2261 | 10,9045 | 11,1378 | 38.0975 | 22.8282 | 18.5625 |
| | | Present | 11.2152 | 10.8959 | 11.1174 | 38.0926 | 22.8264 | 18.5594 |
| | 3 | Trinh *et al.* (2016) | 25,2608 | 24,8745 | 25.4947 | 84.7945 | 51.0434 | 41.5692 |
| | | Present | 25.2537 | 24.8222 | 25.4577 | 84.7839 | 51.0010 | 41.5425 |

Table 6 Fundamental frequency of of *P-P* $Si_3N_4$/SUS304 beams under LTD and NLTD (*L/h*= 20)

| Temperature distribution | Δ*T*(K)=20 | | | 40 | | | 80 | | |
|---|---|---|---|---|---|---|---|---|---|
| | *p*=0.1 | 0.5 | 1 | *p*=0.1 | 0.5 | 1 | *p*=0.1 | 0.5 | 1 |
| LTD (Ebrahimi *et al.* 2015) | 8.4634 | 6.5415 | 5.7114 | 8.2781 | 6.3717 | 5.5469 | 7.8795 | 6.0063 | 5.1927 |
| Chen *et al.* 2018 | 8.4716 | 6.5742 | 5.7588 | 8.2802 | 6.3957 | 5.5847 | 7.8766 | 6.0166 | 5.2128 |
| Present | 8.4685 | 6.5489 | 5.7196 | 8.2768 | 6.3702 | 5.5449 | 7.8727 | 5.9902 | 5.1713 |
| NLTD (Ebrahimi *et al.* 2015) | 8.4675 | 6.5437 | 5.7124 | 8.2911 | 6.3803 | 5.5527 | 7.9265 | 6.0402 | 5.2186 |
| Chen *et al.* 2018 | 8.4730 | 6.5779 | 5.7632 | 8.2837 | 6.4055 | 5.5965 | 7.8861 | 6.0431 | 5.2448 |
| Present | 8.4229 | 6.5098 | 5.6826 | 8.2319 | 6.3357 | 5.5137 | 7.8303 | 5.9691 | 5.1569 |

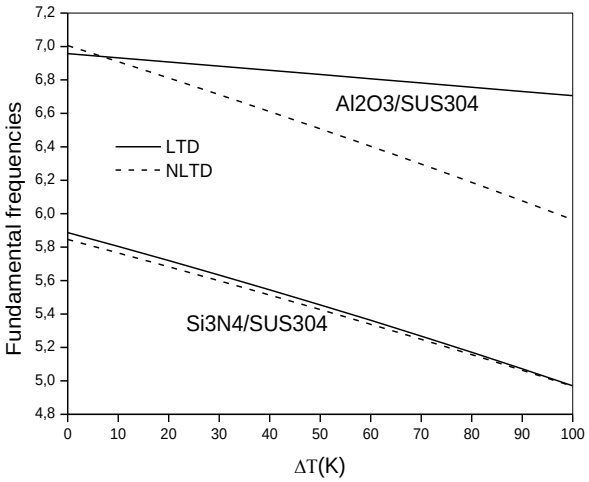


Fig. 5 Fundamental frequencies of FGM beams under LTD and NLTD with different temperature change (*L/h*=20)

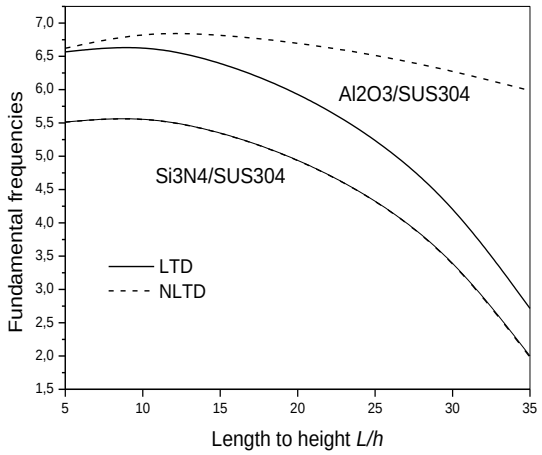


Fig. 6 Fundamental frequencies of FGM beams under LTD and NLTD with different temperature change (Δ*T*=100K), (*L/h*=20)

parameters are depicted in Fig. 4. For this case, a length to height *L/h*=20 and a temperature change Δ*T*=100K are considered. It can be seen that the fundamental frequencies of the FGM beams decrease when the values of the material parameters increase. The differences of the fundamental frequencies between the two temperature distributions are limited. The fundamental frequencies for the NLTD are slightly larger than the LTD ones.

The variations in the fundamental frequencies of the simply FGM beams with respect to temperature change Δ*T* are shown in Fig. 5. A length to height *L/h*=20 and material parameter *p*=1 are considered in this case. As shown in the figure, the fundamental frequencies of FGM beams decrease with the temperature change increasing. Furthermore, the difference in fundamental frequencies for the two temperature distributions is getting larger with the increase of the temperature change.

The relationship between dimensionless fundamental frequency and length-to-height (*L/h*) is plotted in Fig. 6. In this figure, the simply FGM beams made of $Al_2O_3$ /SUS304 and $Si_3N_4$/SUS304 with *p*=1 are taken into consideration. Two types of temperature distribution, LTD and NLTD, with a same temperature change Δ*T*=100K are considered. It can be observed that the dimensionless fundamental frequencies increase first, and then decrease with the increase of the length-to-height ratio. The discrepancy between the LTD and NLTD for the case of FGM beam made of $Al_2O_3$ /SUS304 enlarges slightly with the increase in the length-to-height ratio.

## 5. Conclusions

A refined shear deformation beam theory is proposed to investigate the thermo elastic vibration of FGM beam under thermal loads. Equations of motion derived from Hamilton's principle. The convergence and correctness of the present theory are demonstrated by comparison with the reference data. The effects of the temperature rise, material parameters, thermal moments and slenderness ratios on the free vibration characteristics of FGM beam are studied accordingly. The effects of temperature distribution through the thickness on natural frequencies are also investigated. The present theory is found to be appropriate and efficient in analysing the vibration of FG beams under thermal loads.

## References

Attia, A., Bousahla, A.A., Tounsi, A., Mahmoud, S.R. and Alwabli, A.S. (2018), "A refined four variable plate theory for thermoelastic analysis of FGM plates resting on variable elastic foundations", *Struct. Eng. Mech.*, **65**(4), 453-464. https://doi.org/10.12989/sem.2018.65.4.453.

Bennai, R., Fourn, H., Ait Atmane, H., Tounsi, A. and Bessaim, A. (2019), "Dynamic and wave propagation investigation of FGM plates with porosities using a four variable plate theory", *Wind Struct.*, **28**(1), 49-62. https://doi.org/10.12989/was.2019.28.1.049.

Chen, Y., Jin, G., Zhang, C., Ye, T. and Xue, Y. (2018), "Thermal vibration of FGM beams with general boundary conditions

using a higher-order shear deformation theory", *Compos. Part B*, **153**, 376-386. https://doi.org/10.1016/j.compositesb.2018.08.111.

Ebrahimi, F. and Safarpour, H. (2018), "Vibration analysis of inhomogeneous nonlocal beams via a modified couple stress theory incorporating surface effects", *Wind Struct.*, **27**(6), 431-438. https://doi.org/10.12989/was.2018.27.6.431.

Ebrahimi, F. and Salari, E. (2015), "Nonlocal thermo-mechanical vibration analysis of functionally graded nanobeams in thermal environment", *Acta Astronaut*, **113**, 29-50. https://doi.org/10.1016/j.actaastro.2015.03.031.

El-Haina, F., Bakora, A., Bousahla, A.A., Tounsi, A. and Mahmoud, S.R. (2017), "A simple analytical approach for thermal buckling of thick functionally graded sandwich plates", *Struct. Eng. Mech.*, **63**(5), 585-595. https://doi.org/10.12989/sem.2017.63.5.585.

Giunta, G., Crisafulli, D., Belouettar, S. and Carrera, E. (2013), "A thermo-mechanical analysis of functionally graded beams via hierarchical modeling", *Compos. Struct.*, **95**, 676-690. https://doi.org/10.1016/j.compstruct.2012.08.013.

Hamdi, H. and Farah, K. (2018), "Beam finite element model of a vibrate wind blade in large elastic deformation", *Wind Struct.*, **26**(1), 25-34. https://doi.org/10.12989/was.2018.26.1.025.

Karami, B., Janghorban, M., Shahsavari, D. and Tounsi, A. (2018), "A size-dependent quasi-3D model for wave dispersion analysis of FG nanoplates", *Steel Compos. Struct.*, **28**(1), 99-110. https://doi.org/10.12989/scs.2018.28.1.099.

Menasria, A., Bouhadra, A., Tounsi, A., Bousahla, A.A. and Mahmoud, S.R. (2017), "A new and simple HSDT for thermal stability analysis of FG sandwich plates", *Steel Compos. Struct.*, **25**(2), 157-175. https://doi.org/10.12989/scs.2017.25.2.157.

Mouli, C.B., K. Ramji, Kar, V.R., Panda, S.K., Lalepalli, A.K. and Pandey, H.K. (2018), "Numerical study of temperature dependent eigenfrequency responses of tilted functionally graded shallow shell structures", *Struct. Eng. Mech.*, **68**(5), 527-536. https://doi.org/10.12989/sem.2018.68.5.527.

Rong, X.N., Xu, R.Q., Wang, H.Y. and Feng, S.Y. (2018), "Analytical solution for natural frequency of monopile supported wind turbine towers", *Wind Struct.*, **25**(5), 459-474. https://doi.org/10.12989/was.2017.25.5.459.

Sankar, B.V. and Tzeng, J.T. (2002), "Thermal stresses in functionally graded beams", *AIAA J.*, **40**(6), 1228-1232. https://doi.org/10.2514/2.1775.

Semmah, A., Heireche, H., Bousahla, A.A. and Tounsi, A. (2019), "Thermal buckling analysis of SWBNNT on Winkler foundation by non local FSDT", *Adv. Nano Res.*, **7**(2), 89-98. https://doi.org/10.12989/anr.2019.7.2.089.

Simsek, M. (2010), "Fundamental frequency analysis of functionally graded beams by using different higher-order beam theories", *Nucl. Eng. Des.*, **240**, 697-705. https://doi.org/10.1016/j.nucengdes.2009.12.013.

Sina, S.A., Navazi, H.M. and Haddadpour, H. (2009), "An analytical method for free vibration analysis of functionally graded beams", *Mater. Des.*, **30**, 741-747. https://doi.org/10.1016/j.matdes.2008.05.015.

Trinh, L.C., Vo, T.P., Thai, H.T., T.K. and Nguyen, T.K. (2016), "An analytical method for the vibration and buckling of functionally graded beams under mechanical and thermal loads", *Compos. Part B*, **100**, 152-163. https://doi.org/10.1016/j.compositesb.2016.06.067.

Wattanasakulpong, N., Prusty, B.G. and Kelly, D.W. (2011), "Thermal buckling and elastic vibration of third-order shear deformable functionally graded beams", *Int. J. Mech. Sci.*, **53**, 734-743. https://doi.org/10.1016/j.ijmecsci.2011.06.005.

Wu, H., Kitipornchai, S. and Yang, J. (2018), "Free vibration of thermo-electro-mechanically postbuckled FG-CNTRC beams with geometric imperfections", *Steel Compos. Stuct.*, **39**(3), 319-332. https://doi.org/10.12989/scs.2018.29.3.319.

*CC*